Applied Mathematics and Mechanics
(English Edition, Vol 21, No 11, Nov 2000)

Published by Shanghai University,
Shanghai, China

Article ID: 0253-4827(2000)11-1229-08

SHEAR BEAM MODEL FOR INTERFACE FAILURE UNDER ANTIPLANE SHEAR (Ⅱ) —INSTABILITY*

SHEN Xin-pu (沈新普)[1], Zenon Mroz[2]

(1. Department of Mechanics, Northeastern University, Shenyang 110006, P R China;
2. Institute of Fundamental Technological Research, Polish Academy of Sciences, Warsaw, Poland)

(Communicated by LÜ He-xiang)

Abstract: Based on the (Ⅰ) of the present work, the behavior of shear beam model at crack initiation stage and at instable propagation stage was studied. The prime results include: 1) discriminant equation which clarifies the mode of instability, snap-back or snap-through, was established; 2) analytical solution was given out for the double shear beam and the load-displacement diagram for monotonic loading was presented for a full process; and 3) the problem of the energy release induced by instability was discussed.

Key words: interface layer; antiplane shear; failure; shear beam model; instability; snap-through; snap-back; damage

CLC number: O342 Document code: A

Introduction

The propagation of interlayer cracks and the resulting failure of the interface is one of more important modes occurring in composite materials, rocks and ceramics. A detailed survey of research in this area can be found, for instance, in the articles by Garg[1] or Hutchinson and Suo[2] who discussed mixed-mode crack propagation using the Griffith energy condition. Yang and Ravi-Chandar[3] presented their results for the failure of interface under anti-plane shear action by the Finite Difference Method. However, neither the effects of interface friction nor the instability behavior have been fully investigated.

In the first part of this work, we applied the cohesive crack[3, 4] model assuming the existence of a damage process zone ahead of the crack, and then established the shear beam model for failure of interface. Analytical solution for stable propagation of interface crack was presented in the first part of this work. On the basis of the first part of this work, this paper will investigate the behavior of the shear beam under the joint action of anti-plane shear and lateral compression. The structural behavior for the stage of crack initiation and instable propagation will be studied

* Received date: 1999-08-08; Revised date: 2000-09-20

Foundation item: the EU project (INCO-Compernicus, ERBIC 15 CT970706); Research Foundation for Youth Scientist of Northeastern University, Shenyang, China(856049)

Biography: SHEN Xin-pu(1963～), Associate Professor, Doctor

and also the energy release induced by instability. The analysis will clarify the character of instability points occurring due to interaction of damage zone with the boundary. Analytical solution will be given out for the double shear beam and the load-displacement diagram for monotonic loading will be presented for a full loading process. More complex modes of the interface failure could be treated numerically for different types of loading. In the following text, the meaning of variables is the same as that defined in the first part this work.

1 Rigid Plastic Solution for the Damage Initiation

The initial damage initiation stage occurs when the damage zone starts to develop near the boundary $x = 0$, so we have

$$0 \leq S_2 \leq S_d, \quad w(0) \leq w_c. \tag{1}$$

The shear stress and displacement distribution at the damage initiation stage is the same in form as that expressed in Eq. (28) in the first part of this work, i.e.,

$$\left.\begin{aligned} \tau(x) &= Gr_s[(c_1\sin(r_s x) - c_2\cos(r_s x)], \\ w(x) &= c_1\cos(r_s x) + c_2\sin(r_s x) + \tau_{fc}/K_s, \end{aligned}\right\} \tag{2}$$

where

$$r_s = \sqrt{\frac{K_s}{G}}, \quad c_1 = \frac{\tau_{fc}}{K_s}\cos(r_s S_2), \quad c_2 = \frac{\tau_{fc}}{K_s}\sin(r_s S_2). \tag{3}$$

However, the stress and displacement at the loading end $x = 0$ can not be obtain by Eq. (2) assuming $x = 0$. As taking Eq. (1) into consideration, the equations for the stress and displacement at $x = 0$ are

$$w(0) = c_1 - \tau_{fc}/K_s, \quad \tau(0) = -Gr_s c_2. \tag{4}$$

2 End Zone Solution

Consider now the case when the damage zone reaches the free boundary $S_2 = L$, as that shown in Fig. 3(b). The consecutive damage process is described by assuming increasing S_1 as a control variable with $S_2 = L$. Trial calculation had proved that structure under this condition is at critical state.

2.1 Discussion on the mode of instability

As the damage zone reaches the free boundary $S_2 = L$, the length of damage zone decreases. We shall follow equilibrium path treating $\tau(0)$ and $w(0)$ as variables dependent on S_1. When S_1 reaches L, the damage evolution process is terminated and sliding limit state occurs. It is evident that the derivatives $\mathrm{d}w(0)/\mathrm{d}S_1$ and $\mathrm{d}\tau(0)/\mathrm{d}S_1$ suffer discontinuity when the damage zone reaches the boundary as $S_2 = L$. The derivative $\mathrm{d}\tau(0)/\mathrm{d}w(0)$ also appears discontinuity at this point with consecutive softening or snapback effect.

At the termination of damage zone translation, $S_2 = L^-$ we have,

$$\left.\begin{aligned} &\left(\mathrm{d}\tau(0)/\mathrm{d}S_1\right)_{S_2 = L^-} > 0, \quad \left(\mathrm{d}w(0)/\mathrm{d}S_1\right)_{S_2 = L^-} > 0, \\ &\left(\mathrm{d}\tau(0)/\mathrm{d}w(0)\right)_{S_2 = L^-} > 0, \end{aligned}\right\} \tag{5}$$

where the superscript '-' means the value at $S_2 = L^-$. At the initiation of the end zone damage process, we may express the softening (snap-through) or snap-back effect. In the first case, we have

$$\left.\begin{aligned} &\left(\mathrm{d}\tau(0)/\mathrm{d}S_1\right)^{+}_{S_2=L} < 0, \quad \left(\mathrm{d}w(0)/\mathrm{d}S_1\right)^{+}_{S_2=L} > 0, \\ &\left(\mathrm{d}\tau(0)/\mathrm{d}w(0)\right)^{-}_{S_2=L} < 0, \end{aligned}\right\} \tag{6}$$

and the snap-back case is specified by the inequalities

$$\left.\begin{aligned} &\left(\mathrm{d}\tau(0)/\mathrm{d}S_1\right)^{+}_{S_2=L} < 0, \quad \left(\mathrm{d}w(0)/\mathrm{d}S_1\right)^{+}_{S_2=L} < 0, \\ &\left(\mathrm{d}\tau(0)/\mathrm{d}w(0)\right)^{-}_{S_2=L} > 0. \end{aligned}\right\} \tag{7}$$

The following boundary condition are satisfied for both of these cases

$$\tau(L) = 0, \quad w(S_1) = \frac{(\tau_{\mathrm{fc}} - \mu\sigma_n)}{K_{\mathrm{s}}}. \tag{8}$$

These two types of end-zone solutions are illustrated in Fig. 1.

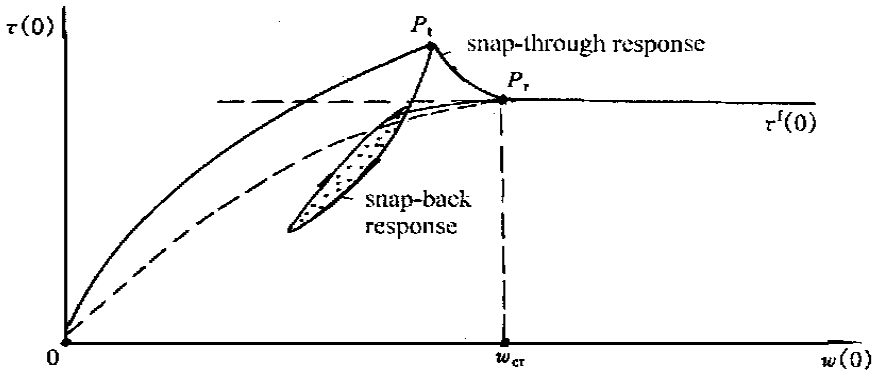

Fig. 1 Illustration of evolution of $\tau(0)$ and $w(0)$ for stable and unstable regimes

2.2 Solution on the equilibrium path of instability

2.2.1 Snap-through solution

Let us first discuss the snap-through solution for which $\tau(0)$ decrease and $w(0)$ increases with increasing S_1, as is specified by the inequalities in Eq. (6). Starting from the general solution of Eq. (1). Within the damage zone, the boundary condition at $x = L$ and at $x = S_1$ are

$$w'(L) = 0, \quad [w(S_1)] = [w'(S_1)] = [W''(S_1)] = 0, \tag{9}$$

and now $\tau_{\mathrm{f}}(L) < \tau_{\mathrm{fc}}$, $w''(L) \neq 0$, constants c_1 and c_2 occurring in Eq. (1) are

$$c_1 = \frac{\mu\sigma_n}{K_{\mathrm{s}}} \frac{\cos(r_{\mathrm{s}}L)}{\cos(r_{\mathrm{s}}\bar{S}_d)}, \quad c_2 = \frac{\mu\sigma_n}{K_{\mathrm{s}}} \frac{\sin(r_{\mathrm{s}}L)}{\cos(r_{\mathrm{s}}\bar{S}_d)}, \quad \bar{S}_d = L - S_1. \tag{10}$$

The stress and displacement fields within the damage zone now are

$$\left.\begin{aligned} \tau(x) &= Gr_{\mathrm{s}} \frac{\mu\sigma_n}{K_{\mathrm{s}}} \frac{\sin[r_{\mathrm{s}}(L-x)]}{\cos(r_{\mathrm{s}}\bar{S}_d)}, \\ w(x) &= \frac{\tau^0_{\mathrm{jc}}}{K_{\mathrm{s}}} + \frac{\mu\sigma_n}{K_{\mathrm{s}}}\left\{1 - \frac{\cos[r_{\mathrm{s}}(L-x)]}{\cos(r_{\mathrm{s}}\bar{S}_d)}\right\}. \end{aligned}\right\} \tag{11}$$

Combining this solution with the state within the slip zone, Eq. (24) in the first part of this work, we obtain

$$\left.\begin{aligned} \tau(0) &= S_1\mu\sigma_n + Gr_s\frac{\mu\sigma_n}{K_s}\tan(r_s\bar{S}_d), \\ w(0) &= \frac{\tau_{jc}^0}{K_s} + \frac{\mu\sigma_n}{2G}S_1^2 + \frac{\mu\sigma_n r_s S_1}{K_s}\tan(r_s\bar{S}_d). \end{aligned}\right\} \tag{12}$$

2.2.2 Discriminant equation for the mode of instability

Let us now calculate the derivatives of $\tau(0)$ and $w(0)$ with respect to S_1. From Eq. (10) and Eq. (12), we obtain these derivatives for the end-zone state, namely:

$$\left(\frac{d\tau(0)}{dS_1}\right)^{-}_{S_2=L} = \mu\sigma_n > 0, \quad \left(\frac{d\tau(0)}{dS_1}\right)^{+}_{S_2=L} = -\mu\sigma_n\sin^2(r_s\bar{S}_d) < 0, \tag{13}$$

$$\left.\begin{aligned} \left(\frac{dw(0)}{dS_1}\right)^{-}_{S_2=L} &= \frac{\tau_{fc}}{K_s}\sin(r_s\bar{S}_d) > 0, \\ \left(\frac{dw(0)}{dS_1}\right)^{+}_{S_2=L} &= \frac{\mu\sigma_n}{K_s}r_s[1 - r_s(L - \bar{S}_d)\tan(r_s\bar{S}_d)]\tan(r_s\bar{S}_d). \end{aligned}\right\} \tag{14}$$

These derivatives are evaluated at the initial stage when the damage zone reaches the boundary $x = L$. It is seen that the second derivative in Eq. (13) is negative, so the response propagating is unstable and not controllable by the applied traction $\tau(0)$. The snap-through or snap-back response depends on the sign of the second derivative in Eq. (14), so we have

$$F = 1 - r_s(L - \bar{S}_d)\tan(r_s\bar{S}_d) > 0 \tag{15}$$

for the snap-through response, and

$$F = 1 - r_s(L - \bar{S}_d)\tan(r_s\bar{S}_d) < 0 \tag{16}$$

for the snap-back response. Fig. 2 presents the domains of snap-through ($F \geq 0$) and snap-back ($F < 0$) responses in the plane r_s-F and S_d-F. The critical state represented by the point P_t in Fig. 2 for which the slope discontinuity occurs and will be called the critical transition point, to make distinction with respect to the limit point where the derivative $d\tau(0)/dS_1$ would vanish. We

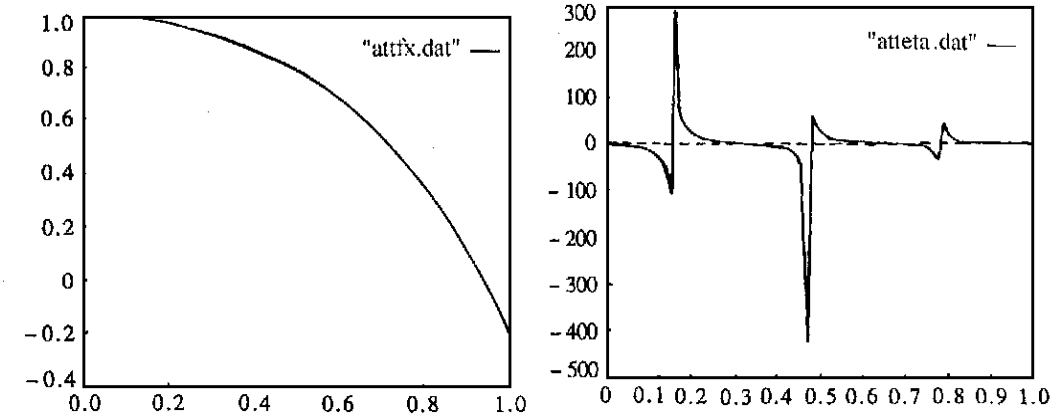

(a) in the plane of r_s-F (b) in the plane of S_d-F

Fig. 2 Domains of snap-through and snap-back responses

also note that when $S_1 = L$, then

$$\left.\begin{aligned} &\left(\frac{\mathrm{d}\tau(0)}{\mathrm{d}S_1}\right)_{S_1=L}=0,\quad \left(\frac{\mathrm{d}w(0)}{\mathrm{d}S_1}\right)_{S_1=L}=0,\\ &\left(\frac{\mathrm{d}\tau(0)}{\mathrm{d}w(0)}\right)_{S_1=L}=0. \end{aligned}\right\} \tag{17}$$

The state when both derivatives of $\tau(0)$ and $w(0)$ with respect to control variable S_1 vanish will be called the terminal state, represented by the terminal point P_r.

2.2.3 Snap-back solution

Let us now calculate the solution for snap-back. Starting from the solution for end zone of Eq. (11). Boundary conditions at $x = L$ and at $x = S_1$ are the same as that described by Eq. (8) and Eq. (9). As the snap-back occurs, reverse sliding appears in certain scope starting from the loading end $x = 0$. Let S_3 denotes the boundary point between reverse slip zone and regular slip zone. The equilibrium equation for reverse slip zone is

$$\frac{\mathrm{d}\tau}{\mathrm{d}x}=-\mu\sigma_n, \tag{18}$$

and then, the solution for reverse sliding zone is

$$\left.\begin{aligned} \tau(x) &= -\mu\sigma_n(x-S_3)+\tau(S_3),\\ w(x) &= \frac{\mu\sigma_n}{G}\left(\frac{x^2}{2}-S_{31}x+\frac{S_3^2}{2}\right)+\\ &\quad \frac{\tau(S_3)}{G}(S_3-x)+w(S_3). \end{aligned}\right\} \tag{19}$$

The boundary condition at $x = S_2$ is

$$[w(S_3)]=[w'(S_3)]=0,\quad [w''(S_3)]\neq 0. \tag{20}$$

The problem following the snap-back phenomena is that how to determine the scope of the region where reverse slip happens. The criteria adopted here for determination of point S_3, which separating the reverse slip zone and normal slip zone, is given in the following equation:

$$\left.\begin{aligned} &\frac{\partial w(x)}{\partial S_1}>0,\quad 0<x<S_3,\quad \text{reverse sliding},\\ &\frac{\partial w(x)}{\partial S_1}=0,\quad x=S_3,\quad \text{stationary point},\\ &\frac{\partial w(x)}{\partial S_1}>0,\quad S_3<x<S_1,\quad \text{regurlar sliding}, \end{aligned}\right\} \tag{21}$$

where $w(x)$ is the displacement field in the frictional slip region which expressed in Eq. (25) in the first part of this work. Eq. (21) implicates that, for a given point of coordinate $x = S_3$, an infinitesimal increment of the position of crack tip S_1 can cause decrease of the displacement for the region up to this point and increase of displacement beyond this point. That is, reverse sliding happens in the region $0 \leq x \leq S_3$, and then the behavior of the structure appears snap-back. According to the solution for monotonic loading expressed by Eq. (25) in the first part of this work, we obtain

$$\frac{\partial w(x)}{\partial S_1}=-\frac{\mu\sigma_n}{G}(S_1-x)+\frac{\tau(S_1)}{G}+\frac{\partial\tau(S_1)}{\partial S_1}\frac{(S_1-x)}{G},$$

$$\frac{\partial \tau(S_1)}{\partial S_1} = Gr_s \left[\frac{dc_1}{dS_1}\sin(r_s S_1) + c_1 r_s \cos(r_s S_1) - \frac{dc_2}{dS_1}\cos(r_s S_1) + c_2 r_s \sin(r_s S_1) \right], \tag{22}$$

where

$$\left.\begin{aligned} \frac{dc_1}{ds_1} &= -\frac{r_s \mu \sigma_n}{K_s}\cos(r_s L)\frac{\sin(r_s \bar{S}_d)}{\cos^2(r_s \bar{S}_d)}, \\ \frac{dc_2}{ds_1} &= -\frac{r_s \mu \sigma_n}{K_s}\sin(r_s L)\frac{\sin(r_s \bar{S}_d)}{\cos^2(r_s \bar{S}_d)}. \end{aligned}\right\} \tag{23}$$

Substitute Eq. (23) into Eq. (22) and assert $x = S_3$. Finally we get

$$\frac{\partial w(S_3)}{\partial S_1} = \frac{\mu \sigma_n r_s}{K_s \tan[r_s(L - S_1)]}\left\{1 - r_s(S_1 - S_3)\tan[r_s(L - S_1)]\right\} = 0. \tag{24}$$

From Eq. (24), we can get the condition for determination of S_3

$$S_3 = S_1 - \frac{1}{r_s \tan[r_s(L - S_1)]}. \tag{25}$$

Having taken into consideration of reverse slip, we get the modified form of Eq. (12)

$$\left.\begin{aligned} \tau(0) &= (S_1 - 2S_3)\mu \sigma_n + Gr_s \frac{\mu \sigma_n}{K_s}\tan(r_s \bar{S}_d), \\ w(0) &= \frac{\tau_{fc}^0}{K_s} + \frac{\mu \sigma_n}{2G}(2S_3^2 - S_1^2) + r_s S_1 \frac{\mu \sigma_n}{K_s}\tan(r_s \bar{S}_d). \end{aligned}\right\} \tag{26}$$

The following Fig. 3(a) shows the variation of S_3 with increasing of S_1 and Fig. 3(b) shows the situation of variation of shear stress at interface layer during snap-back for a given series of loading and boundary conditions.

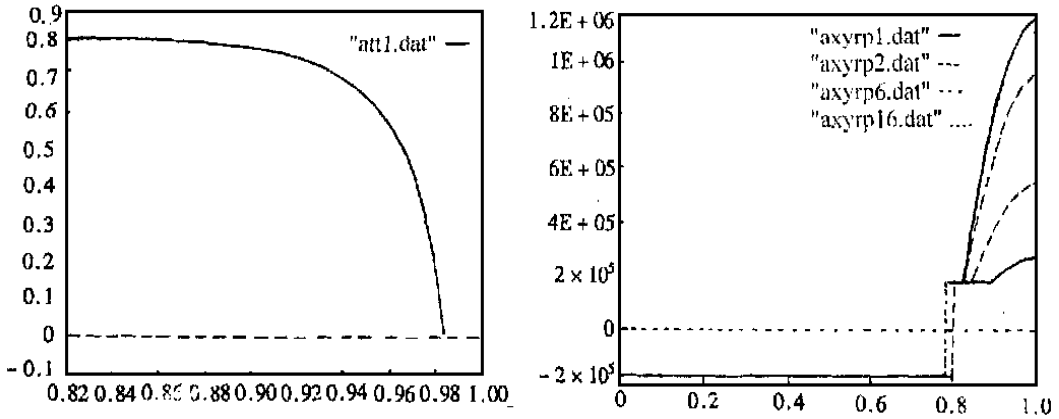

(a) (b)

Fig. 3 (a) Variation of S_3 versus S_1

(b) Variation of $\tau_f(x)$ in the process of snap-back

Combining the solutions for the 3 stage for a monotonic loading process with snap-back, i.e., Eq. (26), Eq. (4) in this paper, and Eq. (34) in the first part of this work, we can get the load-displacement diagram of this rigid-damage-plastic shear beam model, as that shown in Fig. 4(a). The values for parameters adopted in this calculation are

$G = 2.3438 \times 10^9 \text{Pa}$, $\tau_{fc}^0 = 1.0 \times 10^6 \text{Pa}$, $h = 0.16$, $\mu\sigma_n = 0.176 \times 10^6 \text{Pa}$.

For given parameters, the result shown in Fig. 4(a) indicates that the snap-back stage is obvious. The oscillation phenomenon was found by further trial calculation (i.e., the reverse sliding repeatedly appear and vanish during end-stage). Further effort is needed for solution of this problem.

2.3 Discussion on the topic of energy release

The snap-back phenomenon at the end-stage is one kind of structural behavior related to material constitutive properties. The mode of instability is determined by the discriminant equation (Eqs. (15) and (16)). All the three kind of parameters, namely, the material parameters, geometrical parameter, and the external environment parameters such as boundary condition are included in the discriminant equation. This implicates that the snap-back behavior can only happen when all these three kind of parameters are in a certain domain.

The energy released from the system of structure when the instability occurs is an important aspect of the model, because the proper way accounting for energy release is the prerequisite to the application of this model. In Fig. 4(a), the diagram obtained by this model is not the one described by the diagram ADE in Fig. 4(b), which is popular in Ref. [4] about snap-back instability. The loading stress can snap-back to so low a level as that indicated by diagram AC is an important phenomena for the instability related to both the material nonlinearity and geometrical parameter.

The process of snap-back is the process that structure doing work to the external environment which is remarked by the reverse displacement. The work done by the structure to the environment, in another words, the energy released by the structure, is the shadow area of ABCA in Fig. 4(b), and can be calculated as

$$E^R = \int_{(0)_1}^{(0)_2} \tau(0)\, \mathrm{d}w(0), \tag{27}$$

where $w(0)_1$ is the value of displacement at the beginning of snap-back, and $w(0)_2$ is the value of displacement at the end of snap-back. Obviously, the energy released in the process of snap-through is zero.

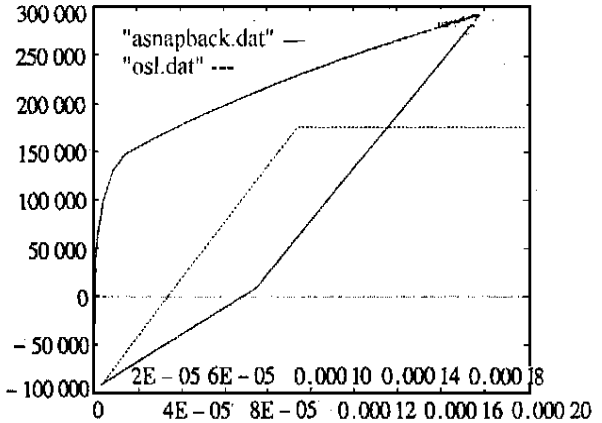

(a)

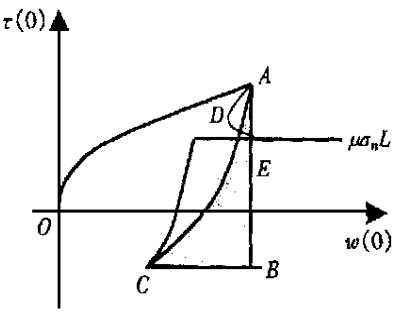

(b)

Fig. 4 (a) The load-displacement diagram for a monotonic loading process
(b) The energy release during snap-back

3 Conclusion and End Remarks

In the first part of this work, the shear beam model for the failure of interface is established. On the basis of the first part of this work, this paper investigates the behavior the shear beam under the joint action of anti-plane shear and lateral compression. The structure behavior for the stage of crack initiation and instable propagation are studied and also the energy release induced by instability. The analysis clarifies the character of instability points occurring due to interaction of damage zone with the boundary and discriminant equation is presented for determination of the mode of instability for a given case. Analytical solution is given out for the double shear beam and the load-displacement diagram for monotonic loading are presented for a full loading process.

References:

[1] Garg A C. Delemination—a damage mode in composite structures[J]. Engng Fract Mech, 1988, **29** (2): 557～584.

[2] Hutchinson J W, Suo Z. Mixed mode cracking of layered materials[A]. In: W Hutchinson, T Y Wu, Eds. Adv Appl Mech[C]. **29**. New York: Academic Press, 1991, 63～191.

[3] Yang B, Ravi-Chandar K. Anti-plane shear crack growth under quasi-static loading in a damaging material[J]. Int J Solids Struct, 1998, **35**(12): 3695～3715.

[4] Widjaja B R. Path-following technique based on residual energy suppression for nonlinear finite element anglysis[J]. Computer an Structure, 1998, **66**(1): 201～209.